Atmospheric Research 228 (2019) 137–151

Contents lists available at ScienceDirect

Atmospheric Research

journal homepage: www.elsevier.com/locate/atmosres

The regional asymmetric effect of increased daily extreme temperature on the streamflow from a multiscale perspective: A case study of the Yellow River Basin, China

Lei Chen[a], Jianxia Chang[a,*], Yimin Wang[a], Shaoming Peng[b], Yunyun Li[a,c], Ruihao Long[a], Yu Wang[b]

[a] State Key Laboratory of Eco-Hydraulics in Northwest Arid Region, Xi'an University of Technology, Xi'an 710048, China
[b] Yellow River Engineering Consulting Co., Ltd, Zhengzhou 450003, China
[c] Institute of Resources and Environmental Engineering, Mianyang Normal University, Mianyang 321000, China

ARTICLE INFO

Keywords:
Streamflow variation
Daily extreme temperature increase scenario
VIC hydrology model
Spatial and temporal scales
Asymmetric effect
Climate elasticity

ABSTRACT

Global warming has caused severe regional water security risks, and from the theory of the hydrological cycle, the daily extreme temperature could also bring an impact on the streamflow volume, which could be even more important than the average temperature. Therefore, based on the level of the maximum or minimum temperature warming scenarios, a variety of meteorological datasets were selected to assess the asymmetric effect of increased daily extreme temperature on the streamflow from a multi-scale perspective by using the Variable Infiltration Capacity (VIC) model. Model simulations indicate that the streamflow experiences more significant changes in response to the maximum temperature than in response to the minimum temperature, and the relationships of streamflow with both the maximum and minimum temperatures show an upwards parabolic response function, but the response function varies with the type of warming. Additionally, the seasonal and monthly duration curves results show that the increases in both the maximum and minimum temperatures demonstrate a similar response that leads the proportion of the flood period streamflow to be increased (*Tmin*: 0.16–0.53%/°C; *Tmax*: 0.11–0.51%/°C). When the minimum temperature increases, the higher the original temperature in the region, the greater the proportion of the flood period streamflow increases. However, when the maximum temperature increases, the opposite effect occurs.

1. Introduction

Against the background of global warming, understanding streamflow variation is critical for regional water security (IPCC, 2013). Global warming will result in changes in temporal (monthly and yearly) and spatial meteorological and hydrological indicators (Dai, 2013; Zhong et al., 2018). Therefore, it is important to clarify the responses of water resources to temperature in a changing environment, particularly under continuous droughts and global warming, for basin-scale water resource planning and management (Tariku and Gan, 2018; Masood et al., 2015). However, the ways in which rising temperatures influence the streamflow at spatial and temporal scales is an area in which researchers generally lack perception and interpretation, especially of the difference between the effects of the daily maximum temperature (*Tmax*) and daily minimum temperature (*Tmin*).

It is generally accepted that global warming is a trend of future climate change. It has been shown in predictions provided by the Intergovernmental Panel on Climate Change that global surface temperatures will rise by 1.8–4.0 °C by the end of the 21st century (Bates et al., 2008). The Paris Agreement also explicitly requests an assessment of the impacts of global warming at 1.5 °C above the preindustrial levels (Rogelj et al., 2016). Research has revealed the critical role of increasing temperatures in the formation mechanism of runoff based on modeling studies of water resources under climate change scenarios (Berg and Sheffield, 2018; Berghuijs et al., 2014). The increases in temperature have immediate as well as long-term effects on streamflow. To date, previous studies accepted two points of consensus: On the one hand, the effect of temperature to runoff is a minor component relative to the precipitation (Miao et al., 2016; Chen et al., 2019), and on the other hand, temperatures can impact the efficiency of the runoff response to precipitation by affecting evapotranspiration and precipitation (Seo et al., 2019; Lambert and Webb, 2008). The scope of this study

* Corresponding author.
E-mail address: chxiang@xaut.edu.cn (J. Chang).

https://doi.org/10.1016/j.atmosres.2019.06.003
Received 25 March 2019; Accepted 7 June 2019
Available online 10 June 2019

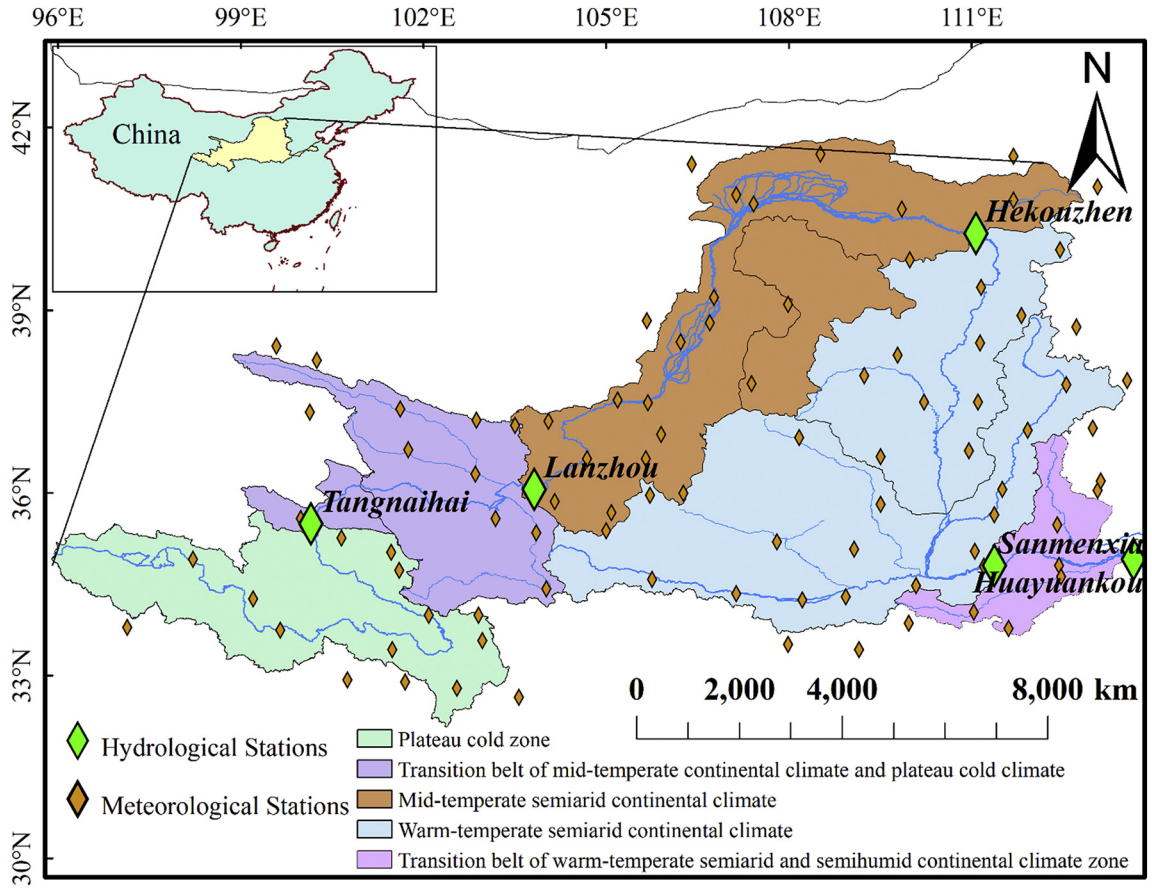

Fig. 1. Map of the Yellow River Basin, which indicates the locations of the meteorological and hydrological stations that were used in this study.

is to focus only on the immediate effect of temperature rises on the streamflow (Vano et al., 2012).

In recent years, the impact of the temperature increase on the water resources of specific regions draw great attention to researchers. Some studies discovered that the streamflow increased as the temperature rose (Arnell, 2003). However, several others studies arrived at the opposite conclusions that streamflow reduced because of temperature increases (Ouyang et al., 2017b). With global warming, the process of snowmelt, infiltration and evapotranspiration will appear with different changes in the trend and degree for different regions. When this change is coupled with different basins that have variable runoff generation characteristics, it is not surprising that the opposite result occurs.

However, regrettably, although much has been written outlining the effects of future temperature increases on streamflow, little previous work has been done to specifically addressed or carried out detailed numerical analysis of climate warming on the water resources of a river basin across different climate and geographic divisions (Thomas and Nigam, 2018; Tang et al., 2012). The majority of previous research has focused on the annual streamflow, and to a lesser degree, on seasonal, monthly and even smaller-scale streamflows (Vano et al., 2015). Furthermore, most of these studies usually focused on the average temperature. And in the formulation of the relevant control global warming goals, researchers also take the change of average temperature as the reference standard. But the fact is, according to the theory of the hydrological cycle, aside from the average temperature, the response of the runoff volume to temperature change is also affected by daily extreme temperature (*Tmax* and *Tmin*) and temperature range, especially in areas of high altitude and extensive temperature variations (Zhang et al., 2014). Meanwhile, in order to simulate atmospheric radiation and evapotranspiration better, the developer creating the model usually uses the daily extreme temperature, not the daily average temperature, as representative temperature elements in physically-based hydrological model (SWAT and VIC, for example). Therefore, the changes of *Tmax* and *Tmin* are the basis of evaluating the climate warming impacts on water resources in a CO_2 doubling environment (Liu et al., 2018; Pingale et al., 2014). Which leaves us a potential problem: How rising daily extreme temperature will change water resources? But unfortunately, the study of this part is still not mature. Especially, scholars seldom discussed the regional asymmetric effect of daily extreme temperature increase to streamflow. Based on the above problems, this study is a comprehensive analysis of increased daily extreme temperatures' impacts on streamflow at annual, seasonal, monthly, and daily scales in different climate and geographic divisions and is important both from science and water management perspectives.

We focus our investigation on the Yellow River Basin (YRB), which has various climatic, soil, and topographic conditions. The streamflow in the region is derived mainly from precipitation, while the groundwater, ice and snow meltwater only play a secondary role in the annual runoff. This basin satisfies the requirements of a comparative analysis of the different geographical, climatic and hydrological conditions when evaluating the effect of increasing temperature on streamflow. The hydrological districts of the Yellow River Basin have a clear temperature gradient from upstream to downstream, which can be divided into different temperature zones. This characteristic can also be used to assess the effects of increased temperature on streamflow in different climate and geographic divisions.

The purpose of this study is to carry out a comprehensive analysis of the sensitivity of streamflow to daily extreme temperature increases from multiple temporal and spatial scale perspective. Specifically, this study discusses separately in detail the regional asymmetric effect of daily extreme temperature increase to streamflow at annual, seasonal and monthly time scales in the YRB and presents a relatively complete

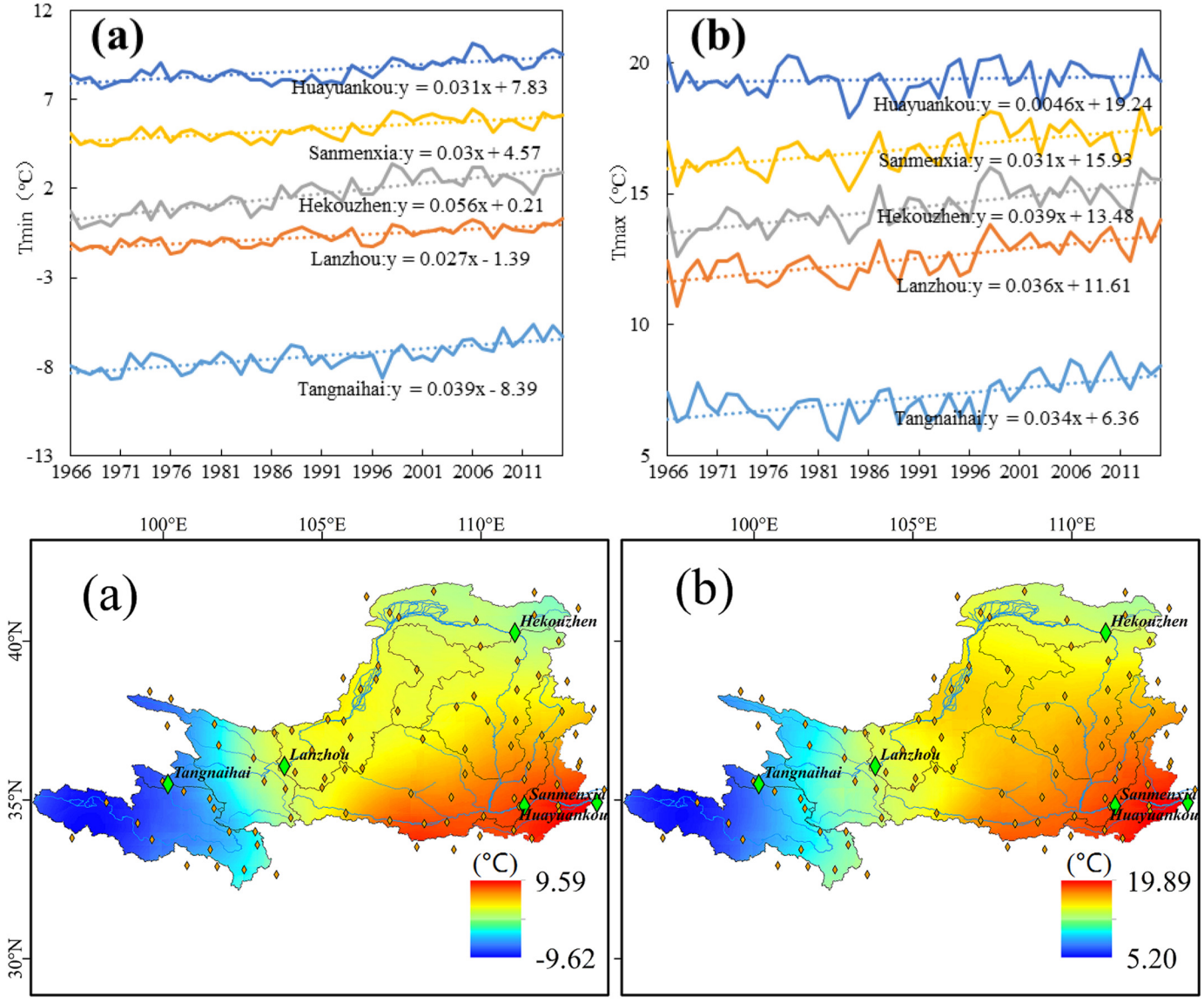

Fig. 2. The spatial distribution and temporal trends in the annual mean of (a) *Tmin* and (b) *Tmax*.

picture of the hydrological processes while considering as many driving scenarios as possible, which is critical to information for the implementation of water resource adaptability policies.

2. Materials and data processing

2.1. Study area

We focus our investigation on the YRB, which runs eastwards across a three-step geographical ladder of China (Tibetan Plateau, Loess Plateau and North China Plain), and covers an area of 752,443 km^2. The amount of natural runoff that is controlled by Huayuankou station is approximately 96% of the total runoff in the Yellow River (Yang et al., 2003; Chang et al., 2019). Since the riverbed is higher than the ground, the downstream Yellow River (Huayuankou-Bo Sea) becomes an aboveground river, and the water-producing area is small. Therefore, the variation trend of the natural runoff at Huayuankou station basically represents the fundamental characteristics of the whole Yellow River Basin. In this paper, the region above Huayuankou is used as the study area, and the following analysis of the YRB is also within this range.

We divided the study area into five parts according to the basin characteristics and the two-grade hydrological districts of China (Fig. 1): (i) the region above Tangnaihai station, which is the source region of the Yellow River in the traditional sense, is located in the northeastern part of the Tibetan Plateau, which belongs to the plateau cold climate region and has the lowest temperature in the basin; (ii) the region between Tangnaihai and Lanzhou stations, which is the transition belt between the mid-temperate continental and the plateau cold climates and the mean temperature in this region is slightly higher than that in the plateau cold climate area; (iii) the region between Lanzhou and Hekouzhen stations, which has a typical high mountain canyon topography and an alluvial plain after the mountain-pass and belongs to the mid-temperate semiarid continental climate; (iv) the region between Hekouzhen and Sanmenxia stations, where the Yellow River flows through the loess plateau and several branches flow into the Yellow River. This area belongs to the warm-temperate semiarid continental climate; and (v) the region between Sanmenxia and Huayuankou stations, which is located in the transition belt of the warm-temperate semiarid and semi-humid continental climate zones. The average temperature in this region is clearly higher than that in the other districts.

2.2. Data processing

We used the monthly streamflow data from the five hydrological stations along the main stream covering the 1966–2010 period to calibrate and verify the hydrologic model throughout the YRB. Water resources in the YRB have been developed and are used to a high degree, thus, the observed runoff of the control hydrological stations cannot reflect the actual state of the river runoff (Liu and Cui, 2011; Yu et al., 2018). As a result, naturalized runoff data, which have been provided by the Yellow River Conservancy Commission (YRCC) and use a unified method for calculating the reductive water quantity, are used to replace the observed runoff to investigate the change in streamflow (Fu et al., 2007; Chang et al., 2018). The unified method for calculating the reductive water quantity consider the following factors: (i) the amount of water directly abstracted from the river channel for irrigation, industry, and domestic use; (ii) the amount of water extra water losses through evaporation and seepage due to dams; (iii) the amount of water transported into and out of the basin; and (iv) the water amount taken via "bypass" channel during flooding events. The daily meteorological data for the study comprise daily precipitation, *Tmax*, *Tmin* and wind speed, which were collected from 1966 to 2015 from 93 Chinese national meteorological observatory stations within the study area and in the surrounding region. The locations of these stations are shown in Fig. 1.

The spatial distribution and temporal trends in the annual mean of daily extreme temperature in the YRB are presented in Fig. 2, which shows that both the *Tmax* and *Tmin* gradually increased from upstream to downstream. This distribution is also consistent with the division of the temperature zones in the YRB. Both the annual mean of *Tmax* and *Tmin* have a significant increasing trends, which indicates that increased temperatures occurred in the YRB and that the temperature will continue to increase in the future due to the impact of global warming. In addition, the increments of *Tmax* and *Tmin* are not completely synchronous, which is why it is the necessity to study the effects of *Tmax* and *Tmin* increase to streamflow separately. Overall, the increasing trend of *Tmin* is larger than that of *Tmax*, especially in the region between Lanzhou and Hekouzhen stations (region iii), which belongs to the mid-temperate semiarid continental climate belt with limited rainfall, strong winds and a large amount of sand. The *Tmin* increase in the region between Tangnaihai and Lanzhou stations (region ii) is unexpectedly lower than that of *Tmax* and displays clear differences compared with that of the other regions. Region ii belongs to the transition belt between the mid-temperate continental climate and the plateau cold climate zones. Therefore, this phenomenon indicates, to a certain degree, that the temperature variability in the transition belt is complex, which agrees with the related study by Vano et al., 2015.

3. Methodologies

3.1. Variable Infiltration Capacity (VIC) model

The Variable Infiltration Capacity (VIC) model (Liang et al., 1994) was applied to simulate the streamflow at a daily time step along with an offline routing model from 1966 to 2015. To numerically evaluate the performance of the model simulations, we used three standard statistical techniques, known as the Nash-Sutcliffe efficiency coefficient (NSE), the percent bias with naturalized streamflow (PBIAS), and the widely used coefficient of determination (R^2) value. Typically, a model simulation is considered to be satisfactory with an NSE > 0.75, −10% < PBIAS < 10%, and R^2 > 0.9.

The VIC model is physically based macro-scale model and uses a spatial uniform network, which has been widely tested and successfully applied to several flow forecasting studies to explore the effects of climate changes studies in many basins (Niu et al., 2013; Tatsumi and Yamashiki, 2015). The model simulates a variety of basic hydrological processes, including precipitation, evapotranspiration, infiltration, melting, migration and accumulation. The grid cell surface runoff by the VIC model were summed downstream using a routing model that generated and transported the runoff to the outlet.

3.2. The elasticity of streamflow changes with the daily extreme temperature

The climate elasticity of streamflow represents the sensitivity of a water system to climate change, and it is usually calculated based on the proportional change in the streamflow to the change in a climatic variable. In recent years, two types of methods have been used most frequently in related studies of climate elasticity: the hydrological modeling simulation and the Budyko hypothesis method (Zhang et al., 2017a; Wang, 2014). The VIC hydrological modeling is used in this study to estimate the hydrological process (Chang et al., 2015). The actual evapotranspiration were consists of three components: canopy evaporation, transpiration and evaporation from bare soils in VIC model, and all of the evapotranspiration components were relation to the potential evapotranspiration. The potential evapotranspiration of the VIC model was calculated using the Penman-Monteith equation.

For the long-term catchment water balance, soil water storage can be neglected, and evaporation can be expressed as a function of precipitation and potential evaporation. Based on the water balance equation,$R = P - E$, we can have $R = f(P, E_0, n)$. R is the long-term average streamflow, while P and E_0 denotes the long-term average of precipitation and potential evapotranspiration, respectively. In addition, the parameter n represents the effect of catchment characteristics, including local topography, soil infiltration, slope, geological structure conditions, and so on. Streamflow changes can be computed by the following differential equation:

$$dR = \frac{\partial f}{\partial P}dP + \frac{\partial f}{\partial E_0}dE_0 + \frac{\partial f}{\partial n}dn \tag{1}$$

In previous studies, Liu et al. (2017) further deduced, in detail, the fractional contribution of many climatic variables to potential evapotranspiration, such as solar radiation, temperature, wind speed and relative humidity:

$$dE_0 \approx \frac{\partial E_0}{\partial Rn}dRn + \frac{\partial E_0}{\partial T}dT_{\max} + \frac{\partial E_0}{\partial T}dT_{\min} + \frac{\partial E_0}{\partial U_2}dU_2 + \frac{\partial E_0}{\partial RH}dRH \tag{2}$$

where Rn, $T_{\max}$, $T_{\min}$, U_2, and RH denote the solar radiation, *Tmax*, *Tmin*, wind speed and relative humidity, respectively.

With the combination of Eqs. (1) and (2), we obtain the following:

$$\frac{dR}{R} = \varepsilon_p\frac{dP}{P} + \varepsilon_n\frac{dn}{n} + \varepsilon_{Rn}\frac{dRn}{Rn} + \varepsilon_{T\max}\frac{dT_{\max}}{T_{\max}} + \varepsilon_{T\min}\frac{dT_{\min}}{T_{\min}} + \varepsilon_{U_2}\frac{dU_2}{U_2} + \varepsilon_{RH}\frac{dRH}{RH} \tag{3}$$

where $\varepsilon_{Rn} = \varepsilon_{E_0}\frac{R_n}{E_0}\frac{\partial E_0}{\partial R_n}$, $\varepsilon_{T\max} = \varepsilon_{E_0}\frac{T_{\max}}{E_0}\frac{\partial E_0}{\partial T_{\max}}$, $\varepsilon_{T\min} = \varepsilon_{E_0}\frac{T_{\min}}{E_0}\frac{\partial E_0}{\partial T_{\min}}$, $\varepsilon_{U_2} = \varepsilon_{E_0}\frac{U_2}{E_0}\frac{\partial E_0}{\partial U_2}$ and $\varepsilon_{RH} = \varepsilon_{E_0}\frac{RH}{E_0}\frac{\partial E_0}{\partial RH}$ denote the elasticity coefficients of solar radiation, *Tmax*, *Tmin*, wind speed and relative humidity to streamflow changes.

Among the factors, only three meteorological factors, that is, precipitation, temperature, and wind, can be measured routinely from a large number of monitoring stations. The other fields, which are extremely hard to measure over a large scale, are mainly calculated by relating them to precipitation and the daily extreme temperature. Thus, excluding any changes in the precipitation and wind speed, the contributions of the *Tmax* and *Tmin* to the change in streamflow can be estimated as:

$$\frac{dR}{R} = \varepsilon_{T\max}\frac{dT_{\max}}{T_{\max}} + \varepsilon_{T\min}\frac{dT_{\min}}{T_{\min}} \tag{4}$$

In this study, the elasticity of streamflow denotes the proportional

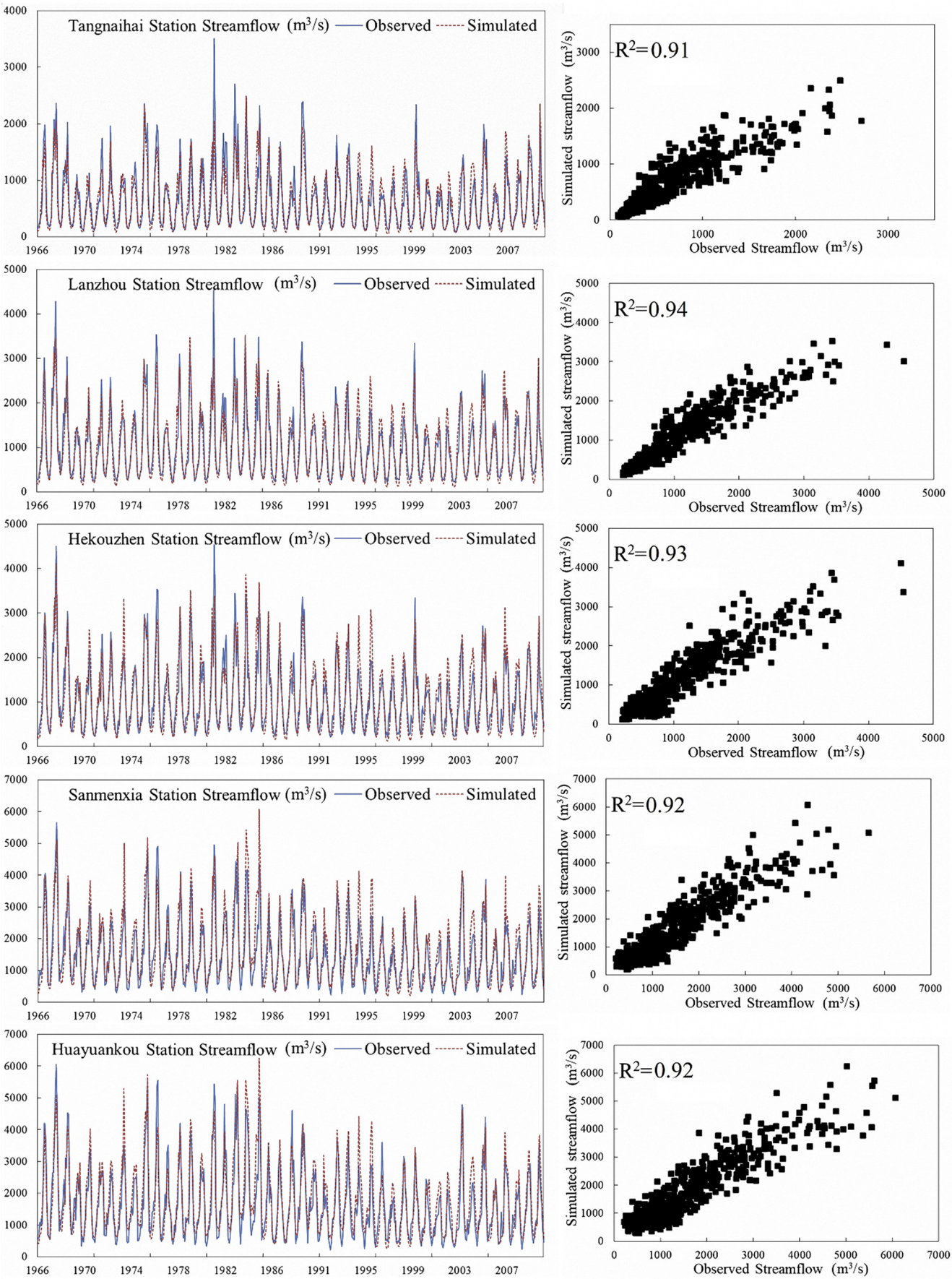

(caption on next page)

Fig. 3. VIC model calibration results for Tangnaihai, Lanzhou, Hekouzhen, Sanmenxia and Huayuankou stations. (Left) The time series curves (1966–2010) of observed (Blue) and simulated (Red) streamflow at selected hydrological stations along the YRB, and (Right) the observed and simulated streamflow scatter plots. (For interpretation of the references to colour in this figure legend, the reader is referred to the web version of this article.)

change in streamflow based on a 0.1 °C increase in *Tmax* or *Tmin* variable. Thus, the elasticity coefficients of *Tmax* and *Tmin* to the streamflow changes are defined as:

$$\varepsilon_{T\max/T\min} = \frac{\Delta R}{\Delta T_{\max/\min}} \frac{T_{\max/\min}}{R} = \frac{\Delta R/R}{\Delta T_{\max/\min}/T_{\max/\min}} \quad (5)$$

where ΔR represents the streamflow changes due to each influencing factor. $\Delta T_{\max/\min}$ denotes the change in temperature in relative values, and $T_{\max/\min}$ is defined as one unit (0.1 °C) of relative change in temperature. The sensitivity of streamflow changes to influencing factors was reflected in the absolute value of elasticity coefficients.

4. Results and analysis

4.1. Model calibration results

Fig. 3 presents the time series curves of observed and simulated streamflow at selected hydrological stations during the reference period (1966–2010), which reflect the performance of the spatiotemporal simulation of the hydrological model. The reference period encompassed a range of wet, dry, and normal years for testing the VIC model's performance. With an appropriate calibration, the VIC model generated satisfactory simulations of monthly streamflow during the 45-year period, indicated by the evaluation indexes with the NSE ranging from 0.79 to 0.88 and the percent bias ranging from −1.2% to 8.7% for the selected stations (Table 1). The visual comparison in Fig. 3 reveals that the model can simulate streamflow cyclical fluctuations pretty well at the monthly timescale (Tang et al., 2012).

4.2. The regional asymmetric effect of increased daily extreme temperature on the streamflow

This section examines the streamflow changes in the YRB at annual, seasonal and monthly time scales under 30 different *Tmax* or *Tmin* warming scenarios, and analyses the regional asymmetric effect of increased daily extreme temperature on the streamflow. To mitigate global warming, in December 2015, the Paris Agreement was approved by nearly 200 countries at the Conference of the Parties of the United Nations Framework Convention on Climate Change (UNFCCC). This agreement emphasized a two-headed temperature goal: holding the increase in the global average temperature should be controlled within 2 °C above preindustrial levels, and pursuing efforts to limit it below 1.5 °C (Rogelj et al., 2016). Under this great background, according to previous studies, in most GCMs scenarios of future climate change, the temperature increase in the Yellow River Basin will not exceed 3 °C for the rest of this century (Chen et al., 2014; Samaniego et al., 2017). Based on the hypothesis of climate warming, to show a relatively complete picture of the streamflow change processes caused by rising temperature, it is necessary to study the asymmetric effect of increased daily extreme temperature on the streamflow by considering the *Tmax* and *Tmin* separately. And the most significant difference between the *Tmin* rise and the *Tmax* rise is that one reduces the intra-day temperature difference and the other increases the intra-day temperature difference. In this study, 30 scenarios were developed independently by increasing the temperature at 0.1 °C in increments up to 3 °C (i.e., with *Tmax*** or *Tmin* ** representing the scenario in which the minimum/maximum temperature increased by **°C), and the verified VIC model was employed to simulate streamflow. The different responses of streamflow to the same level of warming in the daily extreme temperature demonstrate the importance of investigating the daily extreme temperature increases in a consistent manner, instead of focusing on the average temperature only (Donnelly et al., 2017; Su et al., 2017).

4.2.1. Asymmetric effect at the annual time scales

The objective of this section is to present the analysis of the relationship and differences of the annual streamflow variation due to *Tmax* or *Tmin* increases. First of all, the 30 temperature warming scenarios are divided into six groups according to the differences in the degree of increase: T0.1-0.5, T0.6-1.0, T1.1-1.5, T1.6-2.0, T2.1-2.5 and T2.6-3.0. Then, the performances of *Tmax* and *Tmin* warming scenarios on streamflow are each studied, and the relationship between the temperature and streamflow is concluded on the basis of the fitted curves. Finally, induction and comparative research is conducted on the difference between the spatial variation of the climate elasticity of annual streamflow and the daily extreme temperature variation amplitude is analysed.

Fig. 4 illustrates the magnitude response of the 50-yr annual mean streamflow to the daily extreme temperature increases in the 30 climate warming scenarios, it can be concluded that the effects of *Tmax* and *Tmin* increase to annual streamflow under different climate warming scenarios have significant asymmetry. In order to corroborate this finding, we need building an appropriate model to fit variance tendency of annual streamflow. The response relationship between hydrologic elements tends to be non-stationary due to various natural and artificial causes, and based on this, a nonlinear model is more suitable to model the climatic and hydrological variations and uncertainties than a linear model. The polynomial model was chosen in this case study based on the findings of previous studies (Tang et al., 2012). The trend of change in the mean annual streamflow and daily extreme temperature was modeled using the two-order polynomial, and Table 2(a) displays the test results of the fitted two-order polynomials. The relationship of streamflow to the daily extreme temperatures are upwards parabolic response functions, and the response function patterns which vary with station location and the type of extreme temperature. It should be mentioned that the Y-axis of trend line denotes the effect degree of *Tmax* and *Tmin* increase to annual streamflow under different climate warming scenarios and is used to quantify the asymmetry of the influence degrees of *Tmax* and *Tmin*. A larger values on the Y-axis implies greater degree of the effect on annual streamflow. And the slope of trend line represented annual streamflow sensitivity to the daily extreme temperature change. Below we summarized the observed asymmetric effect of increased *Tmax* and *Tmin* on annual streamflow as the

Table 1
Hydrological stations used in the study and the evaluation for simulation results of monthly runoff of VIC model performance.

Hydrological stations	Latitude (°N)	Longitude (°E)	Drainage area (10^3 km^2)	NSE	PBIAS	R^2
Tangnaihai	35.5	100.15	122	0.82	−0.60%	0.91
Lanzhou	36.07	103.82	223	0.88	−1.20%	0.94
Hekouzhen	40.25	111.17	368	0.84	1.20%	0.93
Sanmenxia	34.82	111.37	688	0.79	8.70%	0.92
Huayuankou	34.92	113.65	730	0.81	8.40%	0.92

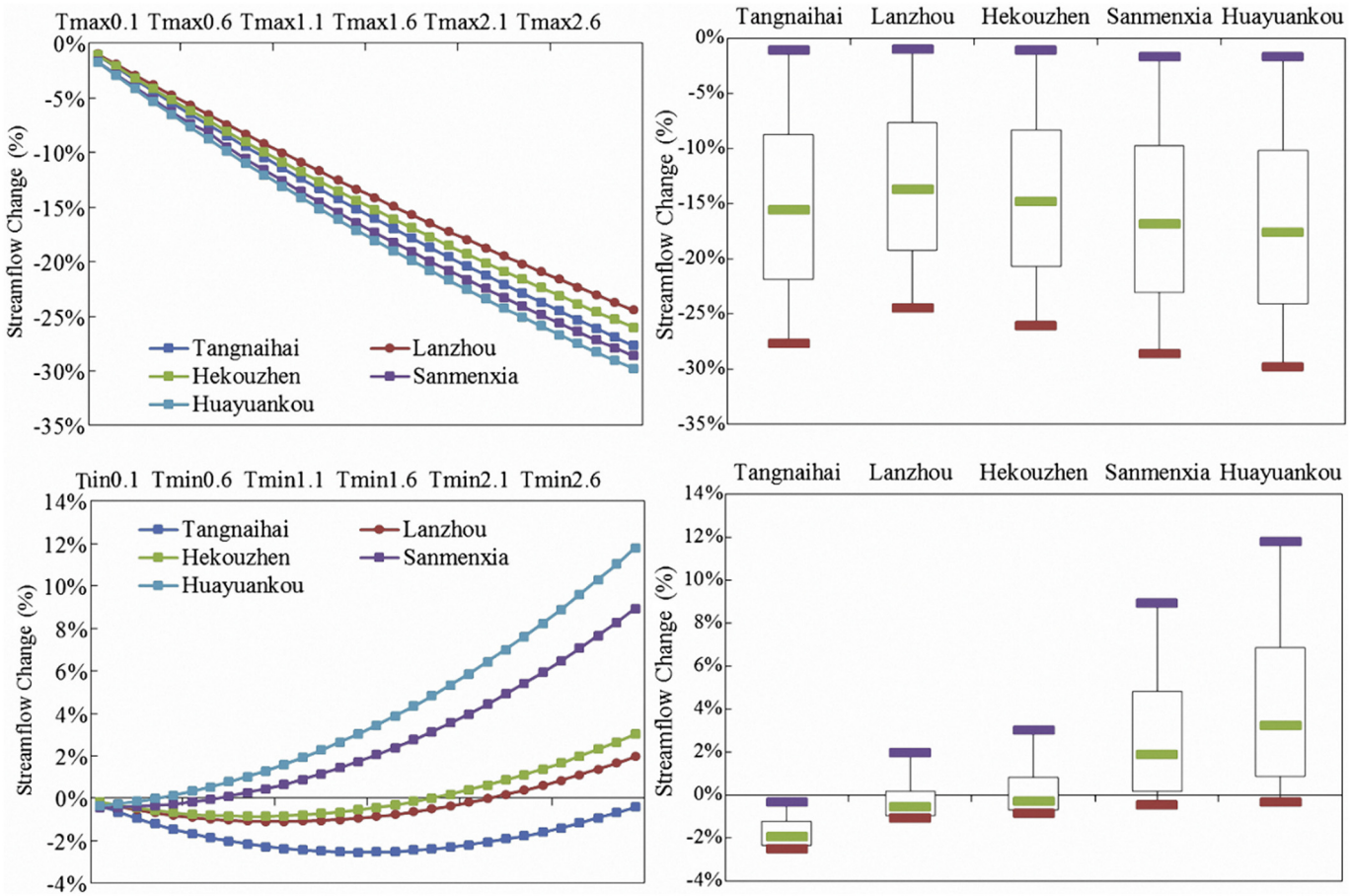

Fig. 4. The magnitude response of the 50-yr annual mean streamflow to the daily extreme temperature increases in the 30 climate warming scenarios.

following two points:

Firstly, the asymmetry of the influence degrees. Different warming scenarios lead to different meteorological conditions. And different meteorological conditions is sure to bring effects to the runoff process. Under the same warming level, the influence of the *Tmax* on annual streamflow is greater than the influence of *Tmin* on annual streamflow. Taking the group T0.1-0.5 as an example, the annual streamflow of multiple hydrological stations is expected to decrease by an average of 3.5% and 0.5% for *Tmax*0.1-0.5 and *Tmin*0.1-0.5, respectively. This result indicate that the annual streamflow was more sensitive to *Tmax* rise than to *Tmin* rise, which agrees with the results of Liu et al. (2017) in studying the impacts of climate element changes on the streamflow using the Budyko hypothesis method. This may be owing to the fact that the *Tmax* has a greater impact on evapotranspiration during hydrological processes, further influencing the annual streamflow. Hence, water resource managers should pay more attention to the changes in *Tmax* under the condition of climate warming.

Secondly, the asymmetry of influence processes. The *Tmax* and *Tmin* warming affects the streamflow of different hydrological stations in very different processes and ways. The annual mean streamflow would continue to decrease at all hydrological stations with the rise of *Tmax*, with the largest decrease occurring from 1.7% (*Tmax*0.1) to 29.8% (*Tmax*3.0) at Huayuankou station and the smallest decrease occurring from 1.0% (*Tmax*0.1) to 24.4% (*Tmax*3.0) at Lanzhou station. The density to sparsity of the changing curve of annual streamflow with the rise of *Tmax*, reveals which the difference between the decrement for the stations continues to increase. However, the influence which climate warming on the annual streamflow was different between the rise in *Tmax* and *Tmin*. With the rise in *Tmin*, the changes in annual streamflow showed a significant upwards parabolic temperature response function and the station closer to the downstream have a larger parabolic curvature. This fitted parabola means that when the magnitude of the increase is small, the streamflow decreases with the increase in *Tmin*, but the rate of decrease continues to decrease. When *Tmin* is increase at a constant rate, the amount of decrease in the streamflow tends to reduce. The streamflow appeared to increase eventually as *Tmin* increased further. Besides, there is a significant spatial distribution to the changes in annual streamflow, which might be attributable to catchment characteristics differences, including local topography, soil infiltration, hydrological, slope, geological structure conditions and original temperature.

To further explore the asymmetry effect of *Tmax* and *Tmin* increase to the annual streamflow in the spatial distribution, we constructed the spatial distribution of the climate elasticity of streamflow as a relative percentage (Fig. 5(a) and (b)). For *Tmin*, the higher the original temperature in the region, the greater the variation in annual streamflow, which is affected by the increase of *Tmin*. Combined with the climatic characteristics of the river basin, it also means that the streamflow changes in the warm-temperate and plateau cold zones were more sensitive to *Tmax* rise than to those in the mid-temperate zone across the YRB. The sensitivity of the streamflow changes to *Tmin* rise across the different temperature zones occurs in the following order: warm-temperate zone > mid-temperate zone > plateau cold zone, and streamflow changes in the downstream were more sensitive to *Tmin* rise than those of area in upstream across the YRB. However, for *Tmax*, the streamflow changes in the warm-temperate and plateau cold zones were more sensitive to *Tmax* rise than were those in the mid-temperate zone across the YRB. These conclusions reflect the larger elasticity coefficients of the streamflow variations in Table 2(b), which are in good agreement with the results of Ouyang et al. (2017a), where lower

Table 2
Annual mean streamflow changes: (a) the relationship between the temperature increase (x) and the mean annual streamflow (y) is displayed as an equation for each station; (b) the elasticity of the daily extreme temperature driving the streamflow (ε_{Tmax} and ε_{Tmin}) at 5 selected hydrological stations in the YRB.

(a)

Change elements	Hydrological stations	The relationship between the temperature increase (x) and the mean annual streamflow (y) is displayed as an equation for each station	R-squared
Tmin	Tangnaihai	$y = 0.0001x^2$-0.0032x0.001	0.9982
	Lanzhou	$y = 0.00008x^2$-0.0018x0.0007	0.9995
	Hekouzhen	$y = 0.00009x^2$-0.0017x0.0003	0.9998
	Sanmenxia	$y = 0.0001x^2$-0.0003x0.0042	0.9999
	Huayuankou	$y = 0.0001x^2 + 0.0005$x0.0039	0.9999
Tmax	Tangnaihai	$y = 0.00006x^2$-0.0109x0.0008	0.9999
	Lanzhou	$y = 0.00005x^2$-0.0096x0.0006	0.9999
	Hekouzhen	$y = 0.00006x^2$-0.0105x0.0006	0.9999
	Sanmenxia	$y = 0.00008x^2$-0.0118x0.0053	0.9999
	Huayuankou	$y = 0.00009x^2$-0.0123x0.0054	0.9999

(b)

Change elements	Hydrological stations	ε_T(%/0.1 °C)					
		T0.1–0.5	T0.6–1.0	T1.1–1.5	T1.6–2.0	T2.1–2.5	T2.6–3.0
Tmin	Tangnaihai	**−0.29**	**−0.16**	**−0.05**	0.05	0.14	0.24
	Lanzhou	**−0.16**	**−0.06**	0.03	0.11	0.19	0.28
	Hekouzhen	**−0.14**	**−0.03**	0.06	0.15	0.24	0.33
	Sanmenxia	**−0.06**	0.14	0.26	0.36	0.48	0.60
	Huayuankou	0.03	0.23	0.35	0.46	0.58	0.71
Tmax	Tangnaihai	−1.08	−1.01	−0.94	−0.88	−0.83	−0.79
	Lanzhou	−0.95	−0.89	−0.83	−0.78	−0.74	−0.70
	Hekouzhen	−1.03	−0.96	−0.89	−0.83	−0.77	−0.73
	Sanmenxia	−1.25	−1.06	−0.97	−0.88	−0.81	−0.75
	Huayuankou	−1.30	−1.11	−1.01	−0.92	−0.84	−0.78

The bold in the table is to emphasize the difference in results between different scenarios at the same station in the case of changing elements.

altitude and latitude areas (usually with higher temperature) experienced larger changes in the runoff than that of higher altitude and latitude areas under the condition of global warming.

4.2.2. Asymmetric effect at the seasonal time scales

Seasonal changes in the streamflow regime strongly affect the use and protection of water resources, which suggests that the response of seasonal hydrologic changes to temperature increase is an important part of the study on hydrological sensitivity. For simplicity, we did not follow the usual method of dividing the year into four quarters, instead, we divided it into the flood (July–October) and non-flood (November–June) periods to highlight the difference in the water quantity. This section first introduces the changes in the magnitude of the seasonal streamflow due to *Tmax* or *Tmin* increases and then analyses the change in the fraction of annual streamflow occupied by flood period streamflow at each hydrological station. The aim is to study the relationship between the characteristics of the annual distribution of the streamflow and the climate warming scenarios, as well as the changing patterns of the flood period streamflow.

Fig. 6 illustrates the relationship between climate warming and the seasonal changes in the streamflow at 5 selected hydrological stations. As expected, the amplitude of streamflow has a strong seasonal signal, and the pattern of the seasonal variability changes with the climate warming. For *Tmax*, the effects of *Tmax* warming on the seasonal streamflow coincide with the annual streamflow results, where the streamflow decreased both during the flood and non-flood periods. Even in terms of the degree of effect, there are still differences in the selection of the hydrological stations and the climate warming scenarios. Meanwhile, the elasticity coefficients can be shown in the slope of trend line, and thus we also obtained some valuable information by compared the slope changes. Under the same *Tmax* warming condition, the elasticity coefficients of the non-flood period become slightly larger than those of the flood period. This may be owing to the fact that the lower average temperature during the non-flood period, and the *Tmax* rise has a greater impact on non-flood evapotranspiration than in flood period with higher average temperatures. In addition, we also discovered that the gap of decrement gradually increases across the YRB from upstream to downstream as *Tmax* increases. This kind of variation would change the annual streamflow distribution, and furthermore changes the proportion of streamflow during the flood period to the annual runoff. Due to the absolute dominance of the flood period streamflow in the mean annual streamflow, the decrease in the streamflow during the flood period contributes to a significant decrease in the mean annual streamflow, and this significant streamflow decrease will increase drought risks. This effect in turn will strongly affect water resources management, by providing significant information for agricultural workers on the storage of extra water to cope with droughts and so that the planting structure can be adjusted.

For *Tmin*, the changes in the streamflow also show an upwards parabolic temperature response function to *Tmin* warming during the flood and non-flood periods. Judging from the curvature of these parabolic response functions, the change in the streamflow during the flood period is more intense, and the intensity increases with the hydrological station from the upstream to the downstream. In most scenarios, the flood period streamflow increases as *Tmin* increases. Taking group *Tmin* 2.6–3.0 as an example, the increase occurred at Huayuankou and Sanmenxia stations, with a 9.6% and 11.2% increase in the flood period streamflow, respectively. This may be owing to *Tmin* rise reduces the intra-day temperature difference, and the changed climatic conditions affect the hydrological processes such as evapotranspiration and infiltration, and reduce the actual evaporation of surface water. Compared with the streamflow during the flood period, the streamflow in the non-flood period changed slowly. Apart from Sanmenxia and Huayuankou stations, which are nearest to the downstream, the remaining stations experience reduced streamflow in the non-flood period within the predefined scenarios. In addition, both also

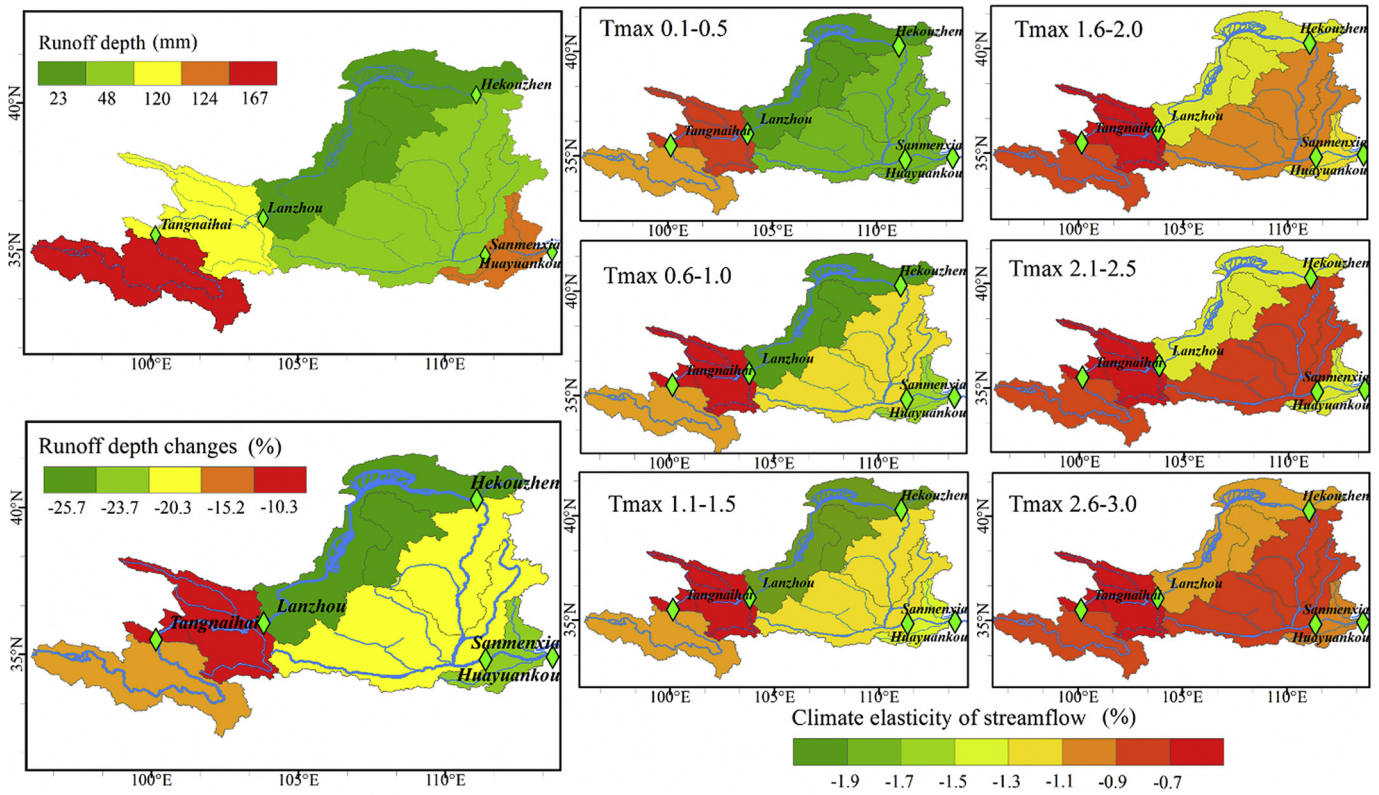

(a)

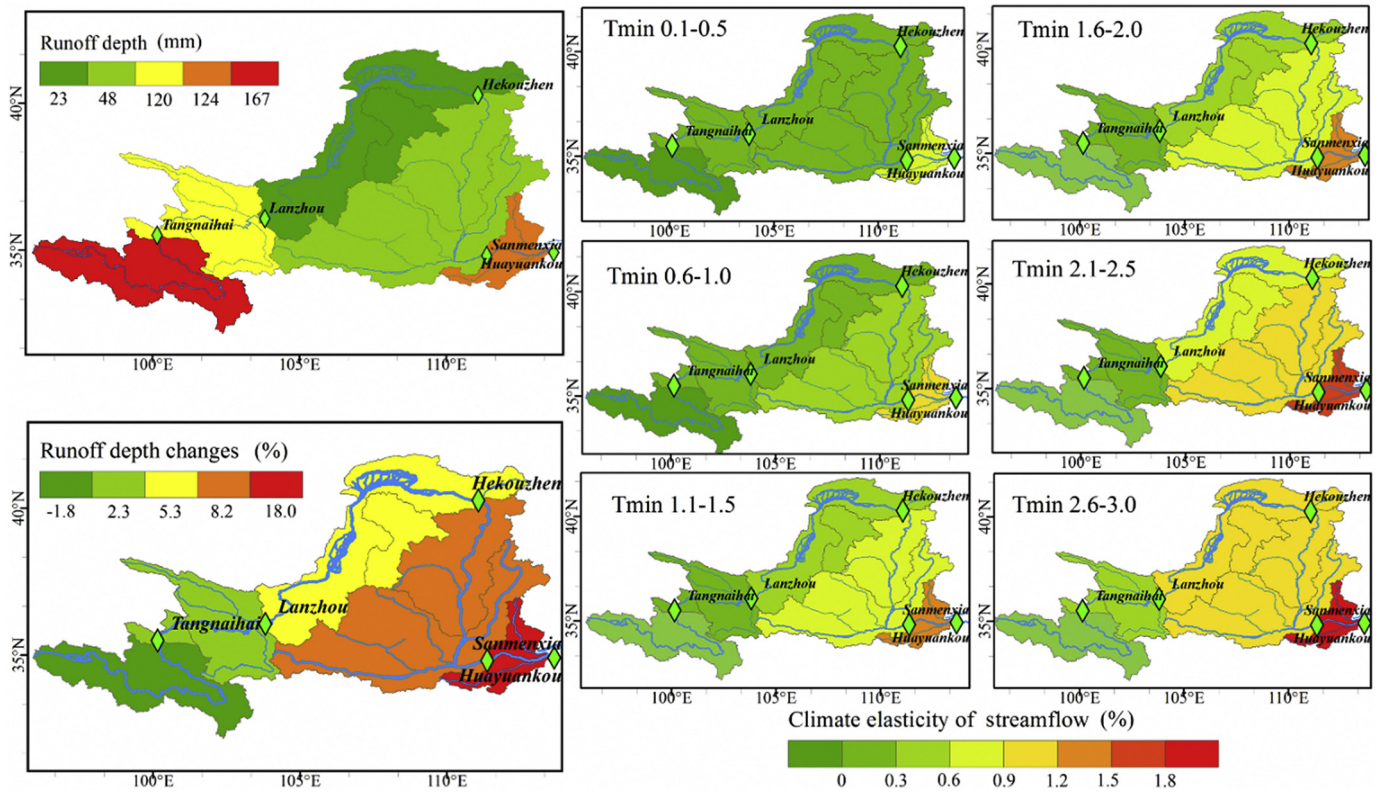

(b)

Fig. 5. The evolution of the spatial distribution of the climate elasticity of annual streamflow (a- *Tmax* and b- *Tmin*) under different climate warming groups. The top figure on the left represent the spatial distribution of runoff depth in the YRB, and the bottom figure on the left represents the spatial distribution of the average runoff depth changes under the 30 *Tmax* or *Tmin* warming scenarios.

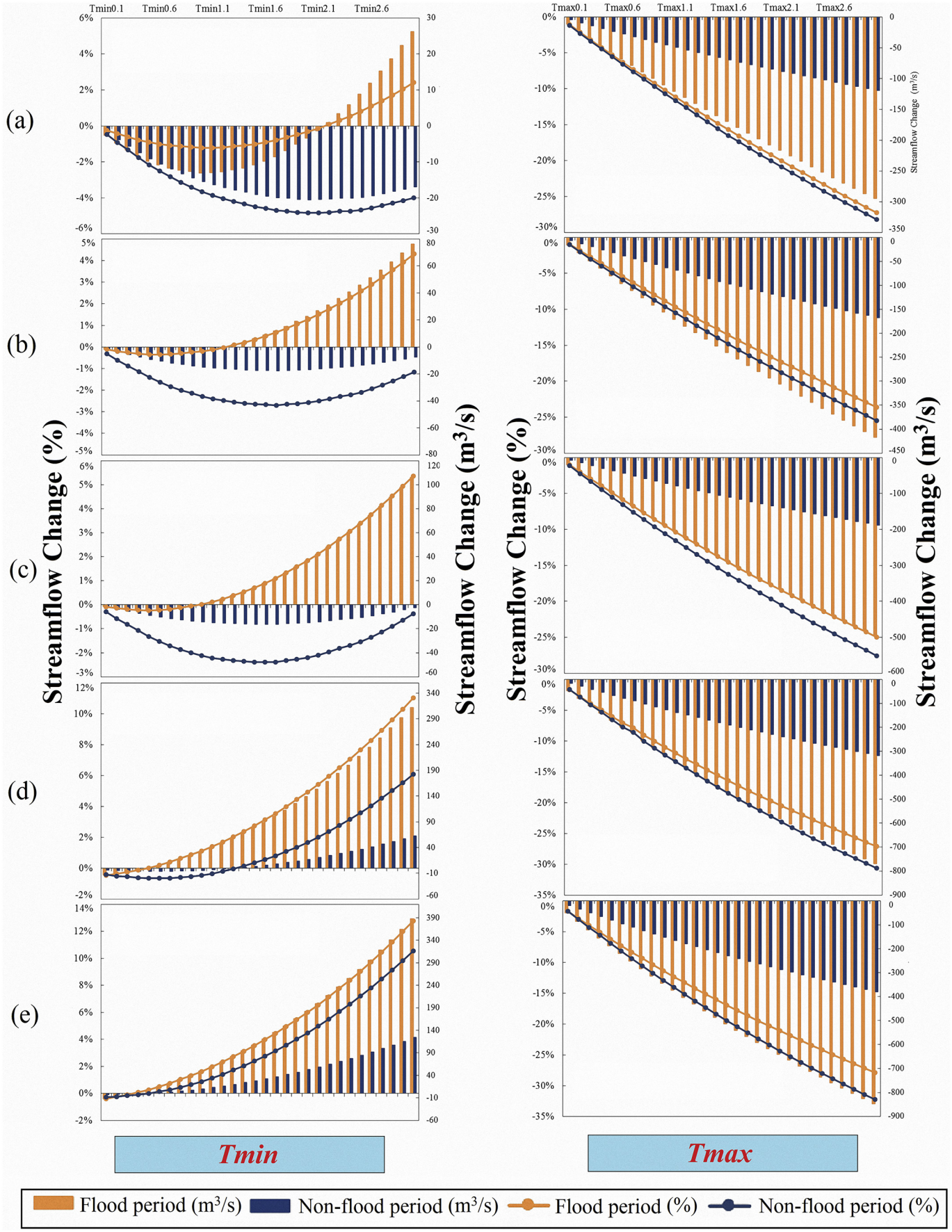

Fig. 6. Relationship between the flood and non-flood period streamflow changes in percent and the temperature increase at 5 selected hydrological stations: (a)-Tangnaihai, (b)-Lanzhou, (c)-Hekouzhen, (d)-Sanmenxia and (e)-Huayuankou. The bar and line charts represent the absolute (m^3/s) and relative (%) value of the streamflow change respectively. (Left) *Tmin* warming scenarios, (Right) *Tmax* warming scenarios.

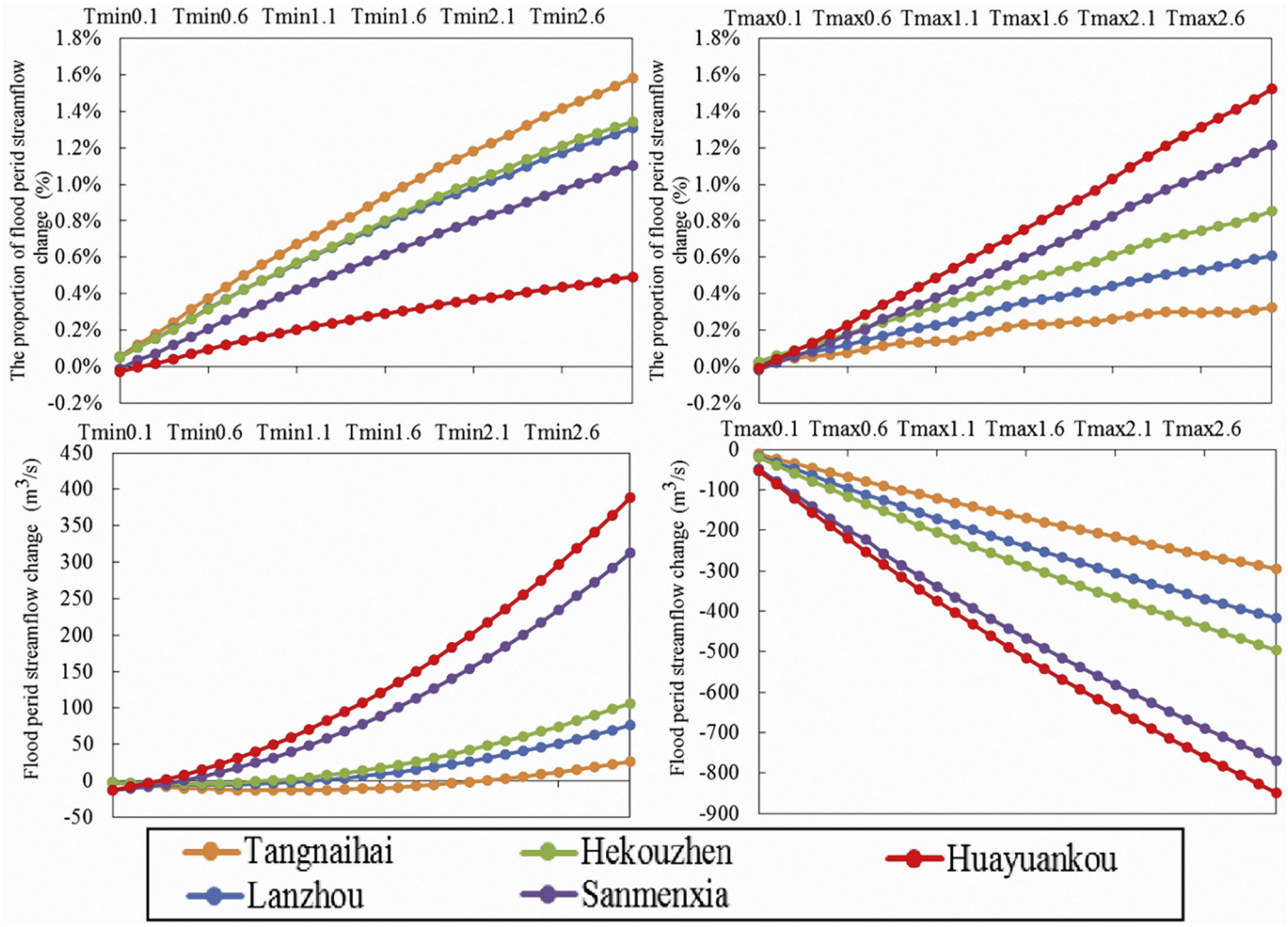

Fig. 7. (Top) The change in the fraction of annual streamflow occupied by flood period streamflow at each hydrological station, and the difference between temperature warming scenarios and the current situation. (Bottom) The absolute change in the streamflow during the flood period.

have an inflection point for the amount of reduction in the *Tmin* 2.0 (Tangnaihai), 1.7 (Lanzhou) and 1.6 (Toudaoguai). The effect of the increase in *Tmin* results in a decrease in the streamflow in the non-flood period, which disappeared from the Sanmenxia station results after *Tmin* 1.4 and from Huayuankou station after the *Tmin* 0.6. This may be owing to the fact that the lower average temperature during the non-flood period, and even *Tmin* in many periods is below 0 °C. In this case, the effect of increased *Tmin* on evapotranspiration was significantly different before and after 0 °C.

To further explore the asymmetric effect of increased daily extreme temperature on the annual distribution of streamflow, we separately analysed the change in the fraction of annual streamflow occupied by flood period streamflow in the two case of increased *Tmax* or *Tmin* (Fig. 7). The increase in *Tmin* and *Tmax* has various effects on the streamflow in the YRB, which causes the amount of streamflow to increase and decrease during the flood period. However, the proportion of streamflow during the flood period with annual streamflow always increases with the increasing temperature, with both *Tmin* and *Tmax*. If *Tmin* rises, the proportion of streamflow during the flood period is expected to increase by 0.16–0.53%/°C, with the largest increase observed at Huayuankou station and the smallest increase at Tangnaihai station. If *Tmax* rises, the proportion of streamflow during the flood period is expected to increase observed by 0.11–0.51%/°C, with the largest increase observed at Tangnaihai station and the smallest increase at Huayuankou station. In addition, there are several other differences worth noting. The higher the original temperature in the region, the greater the proportion of the flood period streamflow increases when *Tmin* increases. However, when *Tmax* increases, the opposite effect occurs.

4.2.3. Asymmetric effect at monthly time scales

From a water management perspective, when producing a water resources regulation scheme, managers are usually not concerned about long-term projects because there is uncertainty and the monthly streamflow changes are more relevant (Chen and Frauenfeld, 2014). The effect of climate warming on streamflow was more significant at a monthly scale than at seasonal or annual scales. Compared to the analysis of the changes at annual and seasonal scales using a similar classification method, the monthly scale data were overly complex. Therefore, the climate warming scenarios were divided into three groups: T0.1–1.0, T1.1–2.0 and T2.1–3.0. We investigated how the monthly streamflow was changed by the temperature increase during the 50-yr study period and evaluated the changes in the high, middle and low flow levels. We also ranked the monthly streamflow series from high to low and presented the duration curve of the streamflow under present conditions and the 6 climate warming groups.

Fig. 8 shows the magnitude response of the 50-yr monthly mean streamflow to the daily extreme temperature increases in the 30 climate warming scenarios. This paper analysed the response of monthly streamflow from two aspects: First, monthly variations in the magnitude response of the streamflow. Affected by the increase in *Tmax*, the magnitude of the streamflow reduction varied between different months. The monthly variety shows the inverted V graphic characteristic, and the months with *Tmax* and *Tmin* amounts of reduction

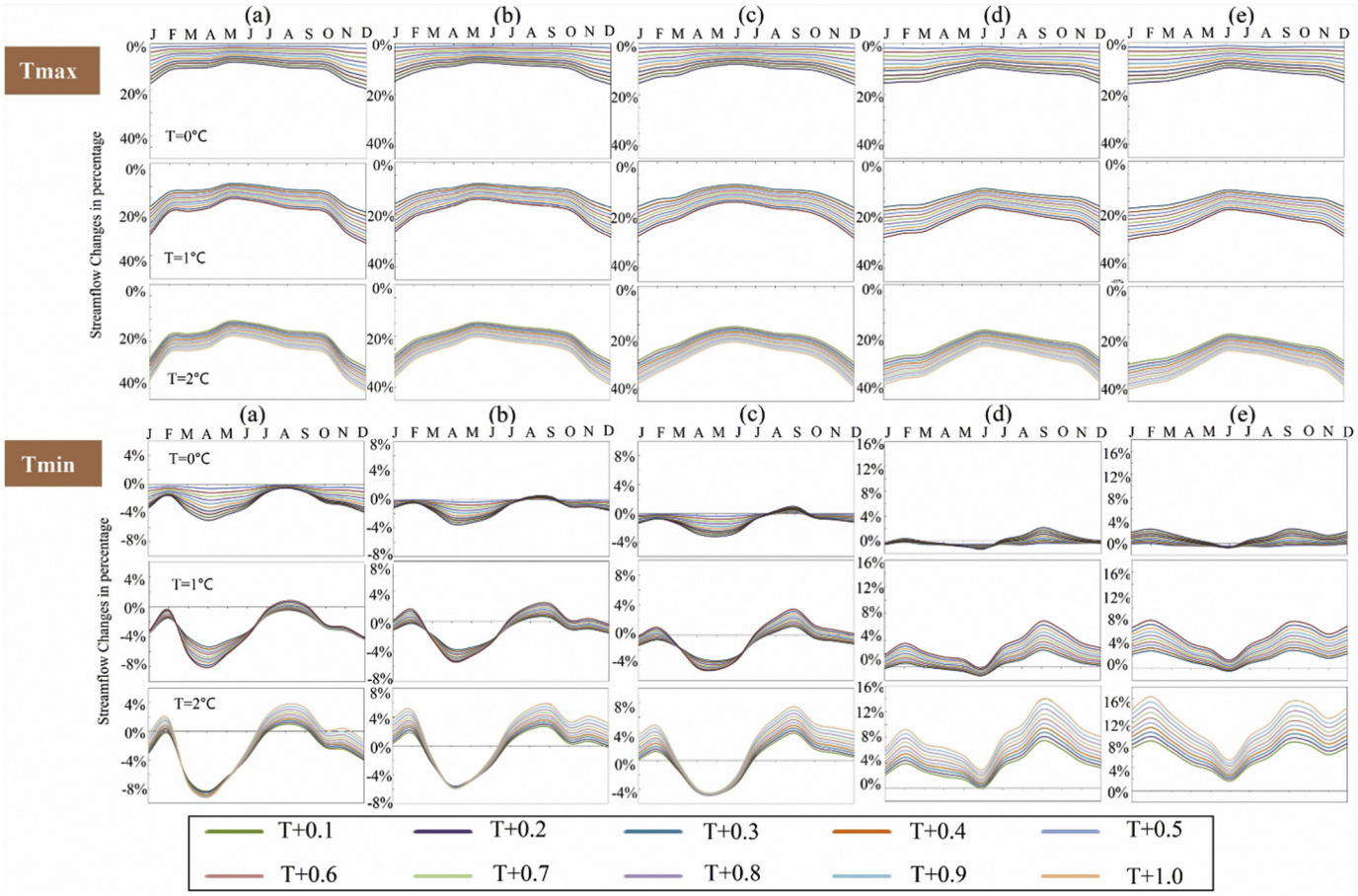

Fig. 8. Relative bias of the monthly streamflow (%) under the 30 temperature scenarios at 5 selected hydrological stations: (a) Tangnaihai, (b) Lanzhou, (c) Hekouzhen, (d) Sanmenxia and (e) Huayuankou. 30 temperature change scenarios are: *Tmax* and *Tmin* increases 0.1 °C per step.

occurred in January and June, respectively. The magnitude of streamflow reduction varied between the different stations, with the greatest decrease occurring at Tangnaihai station from November to January and at Huayuankou station from February to October; Second, scenario variations in the magnitude response of the streamflow can be seen from the density of the changing curve of the monthly streamflow, and the changing curve of monthly streamflow in the *Tmax* 0.1–1.0, *Tmax* 1.1–2.0 and *Tmax* 2.1–3.0 groups became gradually denser. Thus, the effect of *Tmax* on the streamflow decreased with the increasing *Tmax*, and the climate elasticity index of *Tmax* gradually decreased. For example, a three-month continuous streamflow decrease with increasing *Tmax* occurred from May to July at 5 selected hydrological stations, with the smallest change occurring at Lanzhou station when the average decrease in the amount of monthly streamflow was 4.3% (*Tmax* 0.1–1.0), 11.6% (*Tmax* 1.1–2.0) and 18.3% (*Tmax* 2.1–3.0). The continuous maximum decrease over three months occurred from November to January at Tangnaihai and Lanzhou stations and from December to February at Hekouzhen, Sanmenxia and Huayuankou stations, with the greatest change occurring in Huayuankou when the average decrease in the amount of monthly streamflow was 8.9% (*Tmax* 0.1–1.0), 23.0% (*Tmax* 1.1–2.0) and 34.4% (*Tmax* 2.1–3.0).

Compared to *Tmax*, the monthly streamflow changes were clearly different between the 30 *Tmin* warming scenarios. From the monthly variations, the effect of the same *Tmin* increase scenarios on streamflow during the different months varied greatly and was at times the opposite, and showed a distinct response fluctuation graphic characteristic. Taking the *Tmin* 2.0 scenario at Hekouzhen station as an example, the streamflow in May decreased by 4.6%, which is the scenario with the maximum streamflow decrease in the *Tmin* 1.1–2.0 group; and the streamflow in September increased by 3.4%, which is the scenario with the maximum streamflow increase in the group. From the scenario variations, the changing curve of monthly streamflow in the *Tmin* 0.1–1.0, *Tmin* 1.1–2.0 and *Tmin* 2.1–3.0 groups tended to become gradually sparser. This result means that the climate elasticity index of *Tmin* gradually increased and that the effect of *Tmin* on the streamflow increased with the increase in temperature.

Note that there is a particularly striking peak-valley effect as interaction occurs between *Tmin* rise and the quantity of streamflow in the different months. Among them, February, April and September have the most distinct characteristics. When *Tmin* increased and the streamflow decreased, the streamflow in April was the most sensitive to temperature increase and had the largest climate elasticity index. When *Tmin* and streamflow increased, the streamflow in February and September was the most sensitive to the temperature increase. Because of the monthly variability of streamflow, the changes in the mean annual and seasonal streamflows in relation to climate warming were unsurprising.

In addition, with the different types and magnitudes of warming (e.g. *Tmax* or *Tmin*), the mean, high and low flows can produce different degrees and trends of change that affect the streamflow regime. To further explore the changes in the extreme flows, we constructed the duration curves of monthly streamflow (Fig. 9). The duration curve reflects the frequency and quantity of monthly changes in streamflow, especially for high and low flows. The whole duration curve has a descending trend along with a decrease in the overall process flows, which is accompanied by an increase in *Tmax*. The results of the duration curve indicate that the decline in the low flows in the river was even more pronounced than that of the high flows, which led to an

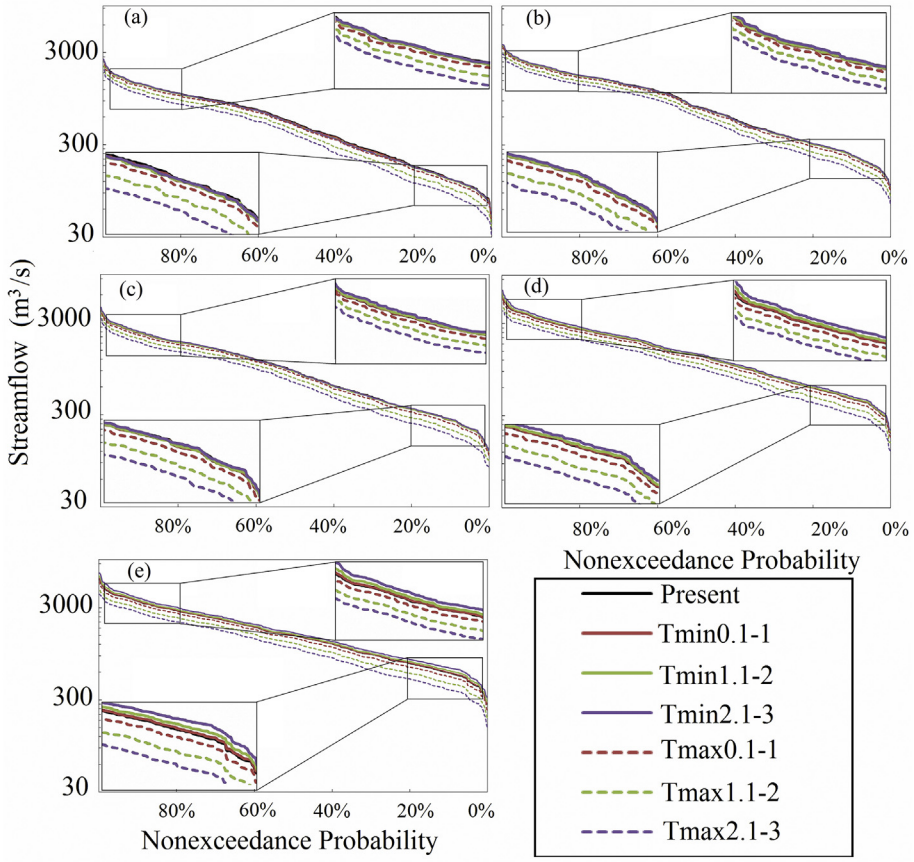

Fig. 9. Duration curve of the Yellow River Basin under the present-day conditions and the 6 temperature scenarios at 5 selected hydrological stations: (a) Tangnaihai, (b) Lanzhou, (c) Hekouzhen, (d) Sanmenxia and (e) Huayuankou.

increase in the slope of the duration curve and the fraction of high flows. This result agrees with the conclusion of the previous section, in that the proportion of streamflow during the flood period with annual streamflow increased with the increasing *Tmax*. While the slope of the duration curve increased slightly along with a slight increase in the high flow and a slower decrease in the low flow, accompanied by increases in *Tmin*, it also increased the proportion of high flow. It is important to note that the result of the increased the proportion of high flow with *Tmax* warming are consistent with *Tmin* warming in the overall trend, but its mechanism of formation is completely different.

5. Discussion

With the appropriate calibration in this study, the VIC generated satisfactory simulations of monthly streamflow during a 45-year period, which was indicated by evaluation indexes NSE of 0.79 to 0.88 and a PBIAS of −1.2% to 8.7% for the selected stations (see Fig. 3 and Table 1). The high R^2 and NSE values calculated during calibration suggest that the calibrated model can be applied to the further study of streamflow variation. A trusted hydrological simulation tool is the basis for all research results in the study (Tan et al., 2017)

The relationships among *Tmax* and annual streamflow is generally stronger than that among annual streamflow and *Tmin*, despite the fact that the increasing trend in *Tmin* was larger than that of *Tmax* in YRB. And the result of this study can be mutually verified with the views of Liu et al. (2017), which used a different research method—the Budyko hypothesis method. The cause of this phenomenon may be owing to the fact that *Tmax* has a greater impact on evapotranspiration during hydrological processes, further influencing the streamflow (Zhang et al., 2017a). Compared with the previous research, we not only study the static characteristics of streamflow caused by daily extreme temperature, but also numerically study the dynamic characteristics and pay more attention to the change process (see Fig. 4). Considering that the most significant difference between *Tmin* rise and *Tmax* rise, that is one reduces the intra-day temperature difference and the other increases the intra-day temperature difference, we can even surmised that the greater the intra-day temperature difference, the stronger the sensitivity of streamflow to daily extreme temperature. But if we want to confirm this inference, then we need to set more scenarios, consider different temperature combinations of *Tmax* and *Tmin*, for further research.

The effect of daily extreme temperature increase to streamflow had obvious seasonal dynamics and spatial distribution, which may explain the different change patterns in the streamflow at 5 selected hydrological stations (see Fig. 5). This may be attributable to catchment characteristics differences, including local topography, soil infiltration, hydrological, slope, geological structure conditions and original temperature (Koster et al., 2012; Huntington and Niswonger, 2012). Of course, there are many disputed and unanswered questions still exist, such as the role of underlying surface in in the process of temperature affecting runoff and the internal mechanism and physical processes of temperature influence on runoff. Further work is needed to resolve these problems in future.

Our research proves that the traditional view of the amplitude of streamflow in YRB has a strong seasonal signal is correct (Hu et al., 2011; Tang et al., 2008), and the increase in *Tmin* and *Tmax* has various effects on seasonal streamflow, which causes the amount of streamflow to increase and decrease during the flood period respectively (see Fig. 6). However, after further research on the streamflow annual distribution in the two case of increased *Tmax* or *Tmin*, we have summed up a new characteristic that the increases in both *Tmin* and *Tmax* demonstrate a similar response that leads the proportion of the flood

period streamflow to be increased (see Fig. 7). After analyzing the duration curves of monthly streamflow, we surmised that this phenomenon may be owing to the fact that the lower average temperature during the non-flood period (Low flows), and the daily extreme temperature rise has a greater impact on non-flood evapotranspiration than in flood period with higher average temperatures.

A major limitation of this study is to focus only on the immediate effect of temperature rises on the streamflow, and ignore the connection between meteorological elements (Zhong et al., 2010). For example, the potential impact of rising temperatures on regional precipitation. In addition, for the convenience of comparative analysis of the asymmetry effect between the *Tmax* and *Tmin*, we artificially split the necessary relation between changes in *Tmax* and changes in *Tmin*, and the increases in *Tmax* and *Tmin* are considered separately in the sensitivity simulations, however this methodology dose not conform to the real world very well (Xu et al., 2011; Zhang et al., 2017b).

6. Conclusions

To conduct a comprehensive analysis of the regional asymmetric effect of increased daily extreme temperature on the streamflow from a multiscale perspective, a hydrological model with as many driving climate warming scenarios as possible was applied to simulate the volume of the streamflow. The Yellow River Basin was taken as an example, and the updated VIC was applied to 5 sub-basins in the Yellow River Basin. After calibrations for streamflow at 5 selected hydrological stations, the model was used to improve the understanding of the correlations between streamflow changes and rising daily temperatures by discussing the asymmetric effect of *Tmax* and *Tmin* increases on the streamflow changes based on 30 different *Tmax* or *Tmin* warming scenarios.

Through the analysis of annual streamflow change of different climate warming scenarios, we summarized the observed asymmetric effect of increased daily extreme temperature on annual streamflow as two aspects, i.e. influence degrees and influence processes. Generally, the relationships of streamflow with both the *Tmax* and *Tmin* show an upwards parabolic response function, and the response function patterns which vary with station location and the type of extreme temperature. The asymmetric variations of increased daily extreme temperature on the streamflow in the spatial distribution can be summarized as follows.① ***Tmin***: The higher the original temperature in the region, the more sensitive the streamflow was to *Tmin* rise. The sensitivity of the streamflow changes to *Tmin* rise occurred in the following order: warm-temperate zone > mid-temperate zone > plateau cold zone; ② ***Tmax:*** When *Tmax* increases, the opposite effect occurs. The streamflow changes in the warm-temperate and plateau cold zones were more sensitive to *Tmax* rise than those in the mid-temperate zone across the YRB. Hence, water resource managers should pay more attention to the changes in *Tmax* under the condition of climate warming, with the understanding that water resources management in downstream is more challenging.

The seasonal and monthly duration curves results show that the increases in both *Tmax* and *Tmin* demonstrate a similar response that leads the proportion of the flood period streamflow to be increased. If *Tmin* increases, the proportion of streamflow in the flood period is expected to increase by 0.16–0.53%/°C; the higher the original temperature in the region, the greater the proportion of the flood period streamflow increases. However, if *Tmax* increases, the amount of streamflow in the flood period is expected to increase by 0.11–0.51%/°C, and the opposite result occurs. Additionally, the monthly duration curve suggest that, when affected by the increase in *Tmax*, the monthly variation in the streamflow shows the inverted V graphic characteristic. However, a striking peak-valley effect of the interaction occurred between *Tmin* rise and the quantity of streamflow in the different months, and the monthly duration curve showed a distinct response fluctuation graphic characteristic.

Given the important role of temperature increases in hydrological cycle processes and the limited focus on daily extreme temperature in previous studies, the present work attempted to fill the knowledge gap on this subject using a hydrological model and independent scenario settings. The results from this study can provide, to a certain extent, a reference to basin-scale water resource management and regional water security.

Acknowledgements

This research is financially supported by the National Key Research and Development Program of China (2017YFC0404404), and the National Natural Science Foundation of China (91647112, 51679187).

References

Arnell, N.W., 2003. Relative effects of multi-decadal climatic variability and changes in the mean and variability of climate due to global warming: future streamflows in Britain. J. Hydrol. 270 (3–4), 195–213.
Bates, B., Kundzewicz, Z., Wu, S., Palutikof, J. (Eds.), 2008. Climate Change and Water. Technical Paper of the Intergovernmental Panel on Climate Change. IPCC Secretariat, Geneva.
Berg, A., Sheffield, J., 2018. Soil moisture–evapotranspiration coupling in CMIP5 models: relationship with simulated climate and projections. J. Clim. 31 (12), 4865–4878.
Berghuijs, W., Woods, R., Hrachowitz, M., 2014. A precipitation shift from snow towards rain leads to a decrease in streamflow. Nat. Clim. Chang. 4 (7), 583–586.
Chang, J., Wang, Y., Istanbulluoglu, E., et al., 2015. Impact of climate change and human activities on runoff in the Weihe River Basin, China. Quat. Int. 380, 169–179.
Chang, J., Wang, X., Li, Y., et al., 2018. Hydropower plant operation rules optimization response to climate change. Energy 160, 886–897.
Chang, J., Guo, A., Wang, Y., et al., 2019. Reservoir operations to mitigate drought effects with a hedging policy triggered by the drought prevention limiting water level. Water Resour. Res. 55 (2), 904–922.
Chen, L., Frauenfeld, O.W., 2014. Surface air temperature changes over the twentieth and twenty-first centuries in China simulated by 20 CMIP5 models. J. Clim. 27 (11), 3920–3937.
Chen, X., Naresh, D., Upmanu, L., et al., 2014. China's water sustainability in the 21st century: a climate-informed water risk assessment covering multi-sector water demands. Hydrol. Earth Syst. Sci. 18, 1653–1662.
Chen, L., Chang, J., Wang, Y., et al., 2019. Assessing runoff sensitivities to precipitation and temperature changes under global climate-change scenarios. Hydrol. Res. 50 (1), 24–42.
Dai, A., 2013. Increasing drought under global warming in observations and models. Nat. Clim. Chang. 3 (1), 52.
Donnelly, C., Greuell, W., Andersson, J., et al., 2017. Impacts of climate change on European hydrology at 1.5, 2 and 3 degrees mean global warming above pre-industrial level. Clim. Chang. 143 (1–2), 13–26.
Fu, G., Charles, S., Chiew, F., 2007. A two-parameter climate elasticity of streamflow index to assess climate change effects on annual streamflow. Water Resour. Res. 43, W11419.
Hu, Y., Maskey, S., Uhlenbrook, S., et al., 2011. Streamflow trends and climate linkages in the source region of the Yellow River, China. Hydrol. Process. 25 (22), 3399–3411.
Huntington, J.L., Niswonger, R.G., 2012. Role of surface-water and groundwater interactions on projected summertime streamflow in snow dominated regions: an integrated modeling approach. Water Resour. Res. 48, W11524.
IPCC, 2013. Summary for policymakers. Climate change 2013. In: Stocker, T.F., Qin, D., Plattner, G.-K., Tignor, M., Allen, S.K., Boschung, J. ... Midgley, P.M.E. (Eds.), The Physical Science Basis. Contribution of Working Group I to the Fifth Assessment Report of the Intergovernmental Panel on Climate Change.
Koster, R.D., Mahanama, P., P, S., 2012. Land surface controls on hydroclimatic means and variability. J. Hydrometeorol. 13 (5), 1604–1620.
Lambert, F.H., Webb, M.J., 2008. Dependency of global mean precipitation on surface temperature. Geophys. Res. Lett. 35, L16706.
Liang, X., Lettenmaier, D.P., Wood, E.F., et al., 1994. A simple hydrologically based model of land surface water and energy fluxes for general circulation models. J. Geophys. Res. 99 (7), 14415–14428.
Liu, Q., Cui, B., 2011. Impacts of climate change/variability on the streamflow in the Yellow River Basin, China. Ecol. Model. 222, 268–274.
Liu, J., Zhang, Q., Singh, V.P., et al., 2017. Contribution of multiple climatic variables and human activities to streamflow changes across China. J. Hydrol. 545, 145–162.
Liu, S., Huang, S., Xie, Y., et al., 2018. Spatial-temporal changes of maximum and minimum temperatures in the Wei River Basin, China: changing patterns, causes and implications. Atmos. Res. 204, 1–11.
Masood, M., Yeh, P.F., Hanasaki, N., et al., 2015. Model study of the impacts of future climate change on the hydrology of Ganges–Brahmaputra–Meghna basin. Hydrol. Earth Syst. Sc. 19 (2), 747–770.
Miao, C., Sun, Q., Duan, Q., et al., 2016. Joint analysis of changes in temperature and precipitation on the Loess Plateau during the period 1961–2011. Clim. Dyn. 47 (9–10), 3221–3234.
Niu, J., Sivakumar, B., Chen, J., 2013. Impacts of increased CO2 on the hydrologic response over the Xijiang (West River) basin, South China. J. Hydrol. 505, 218–227.

Ouyang, W., Gao, X., Hao, Z., et al., 2017a. Farmland shift due to climate warming and impacts on temporal-spatial distributions of water resources in a middle-high latitude agricultural watershed. J. Hydrol. 547, 156–167.
Ouyang, Y., Parajuli, P.B., Li, Y., et al., 2017b. Identify temporal trend of air temperature and its impact on forest stream flow in Lower Mississippi River Alluvial Valley using wavelet analysis. J. Environ. Manag. 198, 21–31.
Pingale, S.M., Khare, D., Jat, M.K., et al., 2014. Spatial and temporal trends of mean and extreme rainfall and temperature for the 33 urban centers of the arid and semi-arid state of Rajasthan, India. Atmos. Res. 138, 73–90.
Rogelj, J., Den Elzen, M., Höhne, N., et al., 2016. Paris Agreement climate proposals need a boost to keep warming well below 2 °C. Nature 534, 631–639.
Samaniego, L., Kumar, R., Breuer, L., et al., 2017. Propagation of forcing and model uncertainties on to hydrological drought characteristics in a multi-model century-long experiment in large river basins. Clim. Chang. 141 (3), 435–449.
Seo, S.B., Bhowmik, R.D., Sankarasubramanian, A., et al., 2019. The role of cross-correlation between precipitation and temperature in basin-scale simulations of hydrologic variables. J. Hydrol. 570, 304–314.
Su, B., Jian, D., Li, X., et al., 2017. Projection of actual evapotranspiration using the COSMO-CLM regional climate model under global warming scenarios of 1.5° C and 2.0° C in the Tarim River basin, China. Atmos. Res. 196, 119–128.
Tan, M.L., Yusop, Z., Chua, V.P., et al., 2017. Climate change impacts under CMIP5 RCP scenarios on water resources of the Kelantan River Basin, Malaysia. Atmos. Res. 189 (1–10).
Tang, Q., Oki, T., Kanae, S., Hu, H., 2008. Hydrological cycles change in the Yellow River basin during the last half of the twentieth century. J. Clim. 21 (8), 1790–1806.
Tang, C., Crosby, B.T., Wheaton, J.M., et al., 2012. Assessing streamflow sensitivity to temperature increases in the Salmon River Basin, Idaho. Glob. Planet. Chang. 88, 32–44.
Tariku, T.B., Gan, T.Y., 2018. Regional climate change impact on extreme precipitation and temperature of the Nile river basin. Clim. Dyn. 51 (9–10), 3487–3506.
Tatsumi, K., Yamashiki, Y., 2015. Effect of irrigation water withdrawals on water and energy balance in the Mekong River Basin using an improved VIC land surface model with fewer calibration parameters. Agr. Water Manage. 159, 92–106.
Thomas, N., Nigam, S., 2018. Twentieth-century climate change over Africa: seasonal hydroclimate trends and Sahara Desert expansion. J. Clim. 31 (9), 3349–3370.
Vano, J.A., Das, T., Lettenmaier, D.P., 2012. Hydrologic sensitivities of Colorado River runoff to changes in precipitation and temperature. J. Hydrometeorol. 13, 932–949.
Vano, J.A., Nijssen, B., Lettenmaier, D.P., 2015. Seasonal hydrologic responses to climate change in the Pacific Northwest. Water Resour. Res. 51, 1959–1976.
Wang, X., 2014. Advances in separating effects of climate variability and human activity on stream discharge: an overview. Adv. Water Resour. 71, 209–218.
Xu, X., Du, Y., Tang, J., et al., 2011. Variations of temperature and precipitation extremes in recent two decades over China. Atmos. Res. 101 (1–2), 143–154.
Yang, D., Li, C., Musiake, K., Kusuda, T., 2003. Analysis of Water Resources in the Yellow River Basin in the Last Century. vol. 280. International Association of Hydrological Sciences, Publication, pp. 70–78.
Yu, Y., Zhang, H., Singh, V., 2018. Forward prediction of runoff data in data-scarce basins with an improved ensemble empirical mode decomposition (EEMD) model. Water 10 (4), 388.
Zhang, X., Tang, Q., Zhang, X., Lettenmaier, D.P., 2014. Runoff sensitivity to global mean temperature change in the CMIP5 Models. Geophys. Res. Lett. 41, 5492–5498.
Zhang, Y., Gao, Z., Pan, Z., et al., 2017a. Spatiotemporal variability of extreme temperature frequency and amplitude in China. Atmos. Res. 185, 131–141.
Zhang, Q., Liu, J., Singh, V.P., et al., 2017b. Hydrological responses to climatic changes in the Yellow River basin, China: climatic elasticity and streamflow prediction. J. Hydrol. 554, 635–645.
Zhong, L., Ma, Y., Salama, M.S., et al., 2010. Assessment of vegetation dynamics and their response to variations in precipitation and temperature in the Tibetan Plateau. Clim. Chang. 103 (3–4), 519–535.
Zhong, R., He, Y., Chen, X., 2018. Responses of the hydrological regime to variations in meteorological factors under climate change of the Tibetan plateau. Atmos. Res. 214, 296–310.